Modeling the metal-semiconductor interaction: Analytical bond-order potential for platinum-carbon

Karsten Albe,* Kai Nordlund, and Robert S. Averback
Frederick Seitz Materials Research Laboratory, University of Illinois at Urbana-Champaign, 104 South Goodwin Avenue, Urbana, Illinois 61801

(Received 4 December 2001; published 13 May 2002)

We propose an analytical interatomic potential for modeling platinum, carbon, and the platinum-carbon interaction using a single functional form. The ansatz chosen for this potential makes use of the fact that chemical bonding in both covalent systems and *d*-transition metals can be described in terms of the Pauling bond order. By adopting Brenner's original bond-order potential for carbon [Phys. Rev. B **42**, 9458 (1990)] we devise an analytical expression that has an equivalent form for describing the C-C/Pt-Pt/Pt-C interactions. It resembles, in the case of the pure metal interaction, an embedded-atom scheme, but includes angularity. The potential consequently provides an excellent description of the properties of Pt including the elastic anisotropy ratio. The parameters for both the Pt-Pt interaction and the Pt-C interaction are systematically adjusted using a combination of experimental and theoretical data, the latter being generated by total-energy calculations based on density-functional theory. This approach offers good chemical accuracy in describing all types of interactions, and has a wide applicability for modeling metal-semiconductor systems.

DOI: 10.1103/PhysRevB.65.195124 PACS number(s): 82.20.Kh, 34.20.Cf, 82.20.Wt

I. INTRODUCTION

Analytical potentials of the embedded-atom type[1–5] represent the current state of art in the classical description of cohesion in metals, and they enable simulations of several million atoms on present day computers. For covalently bonded systems, such as carbon, silicon, and germanium, reactive bond-order potentials play a similar role and have successfully been used in various applications.[6] There are only few simulation studies, however, that considered material processes in mixed covalent-metallic systems. This is due to the lack of analytical potentials that describe the cohesion in metals, carbons, and metal-carbon in a comprehensive way. The modified embedded-atom method (MEAM), as proposed by Baskes[7] provides a possible analytical basis for such a potential, but has not yet been used for carbon. This might be related to the fact that within the MEAM angularity depends only on the atom-type but not on the bond type, so that different hybridizations cannot be easily described. In some studies pair potentials have been used in order to link established semiconductor and EAM potentials.[8–12] The applicability of these approaches, however, is rather limited, since bonds between chemically unsaturated carbon and metal atoms cannot be described.

There is much interest, of course, in material properties and processes that involve chemical interactions between metals and carbon. Typical examples include the growth of nanostructured metallic films on semimetallic inert substrates, such as graphite via cluster beam or vapor deposition techniques. These may be useful for the fabrication of nanoelectronic sensors. The deposition of metal clusters on carbon, or conversely, the deposition of carbon clusters on metals, both at thermal and hyperthermal energies, is also of interest. By metal-cluster deposition an agglomeration of confined quantum systems can be obtained.[13] Diffusion mechanisms of huge clusters on graphite have been identified,[14] and a ''soft landing'' as well as the penetration of metal clusters have been observed.[11] Finally, metals play a dominant role in the synthesis of carbon nanostructures, where they act both as condensation seeds and catalysts.[15] A computationally efficient interatomic potential that realistically describes the structure and chemistry of both covalently bonded materials and metals would therefore be very useful for atomistic simulations of those material processes.

In this study we devise such a potential for carbon-platinum. Platinum is of obvious importance for catalytic devices,[16,17] but there are also several bulk and interface problems related to Pt-C, for instance the optimization of multilayers that are used as the reflector and dispersive element in the optical system of synchrotron beamlines.[18] From a theoretical point of view, carbon and platinum are immiscible systems that do not form a carbide structure.[19] Since the electronegativity difference of Pt and C is small, the charge transfer is negligible. Therefore, this system is an ideal choice for an analytical description using a short–ranged potential.

The paper is organized as follows. First, we show how the bond-order scheme can be linked to established embedded-atom methods, and present the analytical form of the potential. Then the density-functional theory (DFT) calculations, that were performed in order to obtain a set of input data for the parameterization of the potential, are briefly described. Finally, we discuss the fitting procedure for each type of interaction, separately.

II. BASIC METHODOLOGY AND ENERGY FUNCTIONAL

During the past two decades the interest in modeling dynamic processes in condensed phases, where statistical relevance is necessary, has led to the development of many different analytical potentials for various systems that enable large-scale atomistic simulations using molecular dynamics or Monte Carlo methods. These potentials are analytical

functions or functionals, which relate the electronic structure of the system to the lattice topology. Within a quantum-mechanical framework, the tight-binding method is the simplest scheme for describing the energetics of transition metals and semiconductors. This is, therefore, a natural starting point for developing analytical energy functionals. In this section we review the basic assumptions of this theory and derive the analytical functional used in this work.

If we assume only one valence orbital per atomic site, the total energy of the system of interest can be written as:[20,21]

$$E=\frac{1}{2}\sum_{i\neq j}\phi(R_{ij})+\sum_i \underbrace{\int_{-\infty}^{E_f}(E-\epsilon_i)N_i(E)dE}_{V_B^i}. \quad (1)$$

The first term accounts for the repulsion between atomic pairs, and the second is the bond energy calculated as an integral over the local electronic density of states $N_i(E)$ at an atomic site *i*. ϵ_i is the effective atomic energy level. In fact, most structural quantities are insensitive to the details of the electron density of states, being mainly related to its average value and effective width. For *d* transition metals such as platinum, the cohesive energy is dominated by the *d*-band contribution. It is a good approximation, therefore, to assume a rectangular density of states of width W_i, so that the density of states per atom for a full *d*-band will take the value $10/W$. Then the bond energy per site *i* can be written as[21]

$$V_B^i \approx -\frac{1}{20}W_i N_d(10-N_d), \quad (2)$$

where N_d is the number of electrons in the *d*-band.

The width W_i is by definition related to the second moment of the local density of states μ_i^2 via

$$\mu_i^2=\int_{-\infty}^{\infty}E^2N_i(E)dE=\int_{-W_i/2}^{W_i/2}\frac{10}{W_i}E^2dE=\frac{10}{12}W_i^2. \quad (3)$$

On the other hand, the second moment is given by an exact relation, which is the sum of two-center hopping integrals h_{ij}, which depend on the next neighbor distance r_{ij}:

$$\mu_i^2=2\sum_{j(\neq i)}(dd\sigma^2+2dd\pi^2+2dd\delta^2)_{R=R_{ij}}=10\sum_{j\neq i}h^2(r_{ij}). \quad (4)$$

Combining Eqs. (3) and (4) we obtain

$$\frac{1}{12}W_i^2=\sum_{j(\neq i)}h^2(r_{ij}). \quad (5)$$

Finally, using Eq. (5) together with Eq. (2) the total energy in Eq. (1) can be written as a sum over the atomic sites in the following way:

$$E=\frac{1}{2}\sum_i\left(\sum_{j(\neq i)}\phi(r_{ij})-D\underbrace{\sqrt{\sum_{j(\neq i)}h^2(r_{ij})}}_{\rho_i}\right). \quad (6)$$

This is identical to the empirical tight-binding (TB) potentials for transition metals that Cleri and Rosato derived.[22] If we identify the sum over the hopping-integrals as the resulting electron density ρ_i at site *i* and define an embedding function $F(\rho)=D\sqrt{\rho}$, then Eq. (6) corresponds to the Finnis-Sinclair implementation of the embedded-atom method[3–5] as originally proposed by Daw and Baskes.[1,2]

It is appropriate to chose an exponential term for both the distance dependence of the screening function and the hopping integral. Without loss of generality, therefore, we can write $\phi(r_{ij})=A\exp^{-\lambda r_{ij}}$ and $h(r_{ij})=C\exp^{-\mu r_{ij}}$. Equation (6) can then be rewritten as

$$E=\frac{1}{2}\left(\sum_{i\neq j}A\exp^{-\lambda r_{ij}}-\sum_i\underbrace{B\sqrt{\sum_{j(\neq i)}\exp^{-2\mu r_{ij}}}}_{V_B^i}\right), \quad (7)$$

where $B=CD$.

The term V_B^i is the contribution of atom *i* to the band structure energy; it can be rewritten in the following way:

$$V_B^i=B\left(\sum_{j(\neq i)}\exp^{-2\mu r_{ij}}\right)^{1/2} \quad (8)$$

$$=\sum_{j(\neq i)}B\exp^{-\mu r_{ij}}\underbrace{\left[1+\sum_{k(\neq i,j)}\exp^{2\mu(r_{ij}-r_{ik})}\right]^{-1/2}}_{b_{ij}}. \quad (9)$$

If we refer to b_{ij} as the bond-order constant in terms of the Abell-Tersoff concept,[23] then the total-energy expression as derived in Eq. (6) becomes equivalent to a sum over effective bond strengths:

$$E=\frac{1}{2}\sum_{i\neq j}[\underbrace{A\exp^{-\lambda r_{ij}}}_{V_R}-\underbrace{b_{ij}B\exp^{-\mu r_{ij}}}_{V_A}]. \quad (10)$$

This equivalence between the EAM and the bond-order ansatz was previously pointed out by Brenner[24] almost a decade ago. It is basically a consequence of the fact that within the TB approach the chemical bonding of *d* transition metals can be explained in the same terms as those for semiconductors.

Since we have considered only the hopping integrals to the next neighbors, it is necessary and computationally efficient to restrict the interaction to the next neighbor sphere by a cutoff function, which we choose as

$$f(r)=\begin{cases}1, & r\leqslant R-D,\\ \frac{1}{2}-\frac{1}{2}\sin\{\pi(r-R)/(2D)\}, & |R-r|\leqslant D,\\ 0, & r\geqslant R+D.\end{cases} \quad (11)$$

After rearranging the sum, Eq. (10) becomes

$$E=\sum_{i>j}f_{ij}(r_{ij})\left[V_R^{ij}(r_{ij})-\underbrace{\frac{b_{ij}+b_{ji}}{2}}_{\overline{b_{ij}}}V_A^{ij}(r_{ij})\right]. \quad (12)$$

In this present form the bond-order parameter b_{ij}, as defined in Eq. (9), does not include angular dependencies, which are necessary for accurately modeling the deformation of bonds. In order to overcome this deficiency Tersoff introduced angular dependent bond-order functions for silicon, carbon and germanium,[6] while Brenner refined the approach[25] for modeling hydrocarbons. Other closely related potentials were proposed for Si and C (Ref. 26) and, recently, several studies derived analytical bond-order functions directly from a momentum expansion.[27–29] While these approaches differ in the details of their functional form, the resulting angular dependencies of the bond-order are in fact very similar.[29,30] We therefore adopted a straightforward extension developed by Brenner, which is simply an angular dependent term $g(\theta)$ in the inner sum of the bond-order function, so that b_{ij} becomes

$$b_{ij}=(1+\chi_{ij})^{-1/2},$$

$$\chi_{ij}=\sum_{k(\neq i,j)} f_{ik}(r_{ik})g_{ik}(\theta_{ijk})\exp[2\mu_{ik}(r_{ij}-r_{ik})]. \quad (13)$$

Here again the cutoff function is included, while the indices monitor the type dependence of the parameters, which is important for the description of two or more components. The angular function $g(\theta)$ is given by

$$g(\theta)=\gamma\left(1+\frac{c^2}{d^2}-\frac{c^2}{[d^2+(1+\cos\theta)^2]}\right). \quad (14)$$

For $c=0$ this term equals a constant, γ, and the total potential resembles an EAM potential. At this point it is important to recognize that angularity is not only decisive for modeling of covalent systems but also of metals. Alinaghian *et al.*,[27] for example, showed that shear constants can be described in a first-nearest-neighbor potential only if the bond order is angular dependent. In this case, the anisotropy ratio c_{44}/C' can take values smaller than 2.

For convenience, we change the analytical form of the pair-like expressions given in Eq. (10) to the physically more instructive, fully equivalent Morse-like structures

$$V_R(r)=\frac{D_o}{S-1}\exp[-\beta\sqrt{2S}(r-r_o)],$$

$$V_A(r)=\frac{SD_o}{S-1}\exp[-\beta\sqrt{2/S}(r-r_o)], \quad (15)$$

where D_o is the dimer binding energy and r_o the equilibrium distance.

We now have an energy functional that should be suitable for describing Pt-Pt, C-C, and Pt-C within a single formalism as defined in Eqs. (11)–(15). Despite the semiempirical character of this approach, the number of freely adjustable parameters is not more than six for each interaction type, and these can be derived systematically, as follows.

If the binding energy D_o and the ground-state frequency of the dimer molecule are known, then β is simply obtained from the expression

$$\beta=k\frac{2\pi c}{\sqrt{2D_o/\mu}}, \quad (16)$$

where k is the wave number and μ the reduced mass. The parameter S can be determined by the Pauling criterion that relates the equilibrium bonding distance r_b and the energy per bond E_b:

$$E_b=-D_o\exp[-\beta\sqrt{2S}(r_b-r_o)]. \quad (17)$$

When fitting lattice parameters and cohesive energies of structures with different atomic coordinations, Eq. (17) must be fulfilled. This is extremely decisive for the transferability of the potential, as will be shown in the following sections.

III. TOTAL-ENERGY CALCULATIONS

In order to gain insight into the chemistry and bonding, especially of the Pt-C interaction, total-energy calculations were carried out in the framework of the density-functional theory.[31] All results reported here were obtained using the code CASTEP (Ref. 32) with ultrasoft pseudopotentials by Lee (us-PP) and alternatively with norm-conserving pseudopotentials (nc-PP) using the scheme of Troullier-Martin.[33] Exchange and correlation were included using the Perdew-Wang form of the general-gradient approximation (GGA).[34] Calculations of the Pt fcc structure within the local-density approximation (LDA) (Refs. 35 and 36) showed a significant overestimation of the bulk modulus, and therefore they were not used here. This seems to be a shortcoming of the LDA rather than a consequence of using nonrelativistic density functionals for the heavy element Pt, since our nonrelativistic calculations within the GGA are in good agreement with experimental data for fcc Pt.

For all calculated structures the cutoff energies and k-points were chosen to achieve a convergence better than 0.01eV/atom. Total energies for platinum in the fcc, bcc, sc, and diamond structures were calculated. Stoichiometric PtC was investigated in the $B2$ structure (CsCl), the $B1$ structure (NaCl), and in a zinc-blende lattice. The minimum energy, lattice constant, bulk modulus, and pressure derivative of the bulk modulus were calculated by fitting the Birch-Murnaghan equation of state to energy-volume data.[37,38]

IV. CARBON

For modeling the interaction of pure carbon we adopted the C-C parameters given in Brenner's original hydrocarbon potential.[25] Since Brenner proposed two different parameter sets, we compared the Pauling relation [Eq. (17)] to experimental data and DFT calculations available in the literature.[39] Brenner's parameter set I delivers an excellent fit for both the graphite and diamond structures, whereas set II yields a bond length for graphite that significantly deviates from the experimental data, as illustrated in Fig. 1. The overall correspondence to the bond-order relation, however, is better for parameter set II. Since this latter parameterization has a square-root-dependent bond-order, it is fully equivalent to the ansatz chosen for the potential in this study and there-

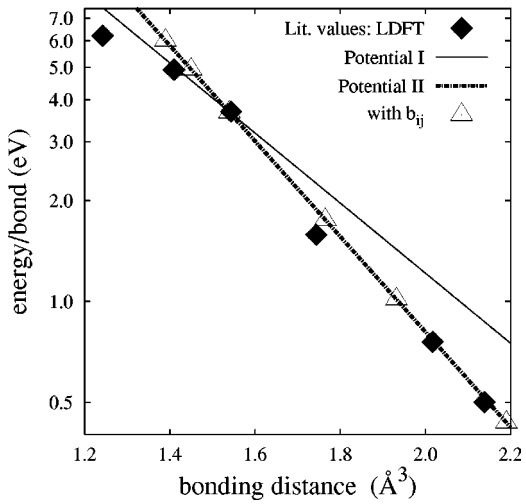

FIG. 1. Comparison of the Pauling energy-bond relation as given by the Brenner potential (Ref. 25) to literature data. Starting from left, the solid data points refer to experimental data for C_2, graphite and diamond, as well as theoretical values from LDFT calculations (Ref. 39) for carbon in sc, bcc and fcc structures. The open points represent the corresponding values obtained by the full potential for carbon.

fore used here. The corresponding C-C parameters are listed in Table V. Additional information can be found in the original paper.

A specific feature of Brenner's potential is the overbinding term, which corrects the unphysical interpolation of single- and double-bonds for some atomic configurations. It is therefore customary to replace the bond-order function by the corrected version

$$\overline{b_{ij}} = \frac{b_{ij}+b_{ji}}{2} + F_{ij}, \tag{18}$$

as described in Ref. 25. Since this correction affects only interactions of pure carbon, we consider the overbinding correction as a necessary option to use in all applications where chemical bonds between carbon atoms of different coordinations become important. In those cases where only ideal carbon structures are involved, this correction might be left out.

Finally, we compared the structural data obtained by CASTEP to other calculations and experiments in order to verify the chosen pseudopotential method for carbon. Apart from the bulk modulus, the results achieved by the norm-conserving pseudopotentials are in excellent agreement with experimental data (see Table I). With the ultrasoft pseudopotentials the bulk modulus is closer to the experimental value, but the lattice constant is slightly too low. Altogether, the calculations agree very well with data obtained with a similar method,[39] and thus serve to validate our choice of pseudopotentials for carbon.

V. PLATINUM

A thorough set of experimental data on the thermomechanical properties of Pt is available. Platinum, however, does not exhibit solid structures other than the fcc phase, so that detailed information on the bonding behavior in undercoordinated environments is not experimentally accessible. We investigated, therefore, the bonding of several hypothetical solid structures with different coordinations by means of DFT calculations using both norm-conserving and ultrasoft pseudopotentials together with nonlocal gradient corrections in the exchange and correlation functionals.

From the total-energy calculations, lattice constants, bulk moduli and cohesive energies were extracted. As shown in Table II the energy differences calculated with both types of pseudopotentials are fully consistent, while the bond lengths calculated with the norm-conserving pseudopotentials tend to be generally larger. The lattice constant for the fcc structure is about 2% too high for the nc-PP and somewhat closer to the experimental value for the us-PP. After rescaling all bond lengths to the experimental value of the Pt fcc phase, the calculations yield consistent data for all structures.

In order to rationalize whether the analytical potential as presented before is capable of describing energy and bonding of Pt, the Pauling relationship [Eq. (17)] was examined. Here the quantities β, r_o, and D_o are in principle given by the dimer properties, and therefore only S is an adjustable parameter. The literature values that can be found for Pt_2 dimer properties are, however, fairly diverse (see Table II). We therefore allowed the dimer properties to vary within the limits of the literature values, and found that the best fit could be obtained for a dimer bond distance of 2.384 Å which is in line with the theoretical values (2.39–2.40 Å). The bond strength was chosen to be close to the average of

TABLE I. Diamond structure calculated within the DFT GGA using ultrasoft pseudopotentials and density mixing, as well as Troullier-Martins pseudopotential with all band minimalization. Results of the LDFT calculation by Furthmüller *et al.* are given for comparison (Ref. 39).

Diamond	LDFT (Ref. 39)	nc-PP GGA-DFT	us-PP GGA-DFT	Expt
V (Å^3)	5.498	5.674	5.531	5.673
a_o (Å^3)	3.530	3.567	3.539	3.567
r_b (Å^3)	1.528	1.544	1.532	1.544
B (GPa)	460	425(1)	439(1)	443
B'	3.64	3.66(2)	3.63(2)	

TABLE II. Calculated structural and cohesive properties of Pt in various phases: Given are volume per atom V, lattice constant a_o, cohesive energy per atom E_{coh}, cohesive energy per bond E_b, bond length r_b, and pressure derivative of bulk modulus B'. Compared are theoretical results, experimental numbers, and the predictions of the analytical potential. DFT calculations were done within the GGA using CASTEP with ultrasoft pseudopotentials and density mixing, as well as the Troullier-Martins pseudopotential with all-band minimalization. Reference data for the Pt_2 dimer were taken from the literature as indicated.

	Theory		Experiment		Analytical Pot.
	Yang *et al.* (LDA-DFT) (Ref. 56)	Varga *et al.* (RDFT) (Ref. 57)	Tayler *et al.* (Ref. 58)	Gupta *et al.* (Ref. 59)	
Pt_2					
r_b (Å^3)	2.40	2.39		2.34	2.384
E_{coh} (eV)	1.65	1.97	1.57	1.855	1.8415
E_b (eV)	3.3	3.94	3.14	3.71	3.683
ω_o (cm^{-1})	218	234	218	259	236
Diamond	nc-PP GGA-DFT	us-PP GGA-DFT			$b_{ij}=0.7761$
V (Å^3)	24.48(2) [23.14] [a]	24.65(5) [23.81]			24.51
a_o (Å^3)	5.807 [5.699]	5.821 [5.753]			5.811
r_b (Å^3)	2.515 [2.468]	2.521 [2.491]			2.516
E_{coh} (eV)	−4.703	−4.587			−4.662
E_b (eV)	−2.352	−2.294			−2.331
B (GPa)	123(1)	117(1)			115.3
B'	5.31(2)	5.57(8)			5.15
SC					$b_{ij}=0.6348$
V (Å^3)	18.66 [17.62]	18.44(5) [17.80]			17.99
a_o (Å^3)	2.652 [2.602]	2.642 [2.611]			2.621
r_b (Å^3)	2.652 [2.602]	2.642 [2.611]			2.621
E_{coh} (eV)	5.296	−5.277			−4.866
E_b (eV)	−1.765	−1.759			−1.622
B (GPa)	182(3)	183(2)			177.6(2)
B'	5.32(6)	5.53(4)			5.39
bcc					$b_{ij}=0.5661$ [b]
V (Å^3)	16.25(2) [15.37]	15.86(2) [15.30]			14.81
a_o (Å^3)	3.192 [3.133]	3.166 [3.128]			3.094
r_b (Å^3)	2.765 [2.713]	2.741 [2.709]			2.680
E_{coh} (eV)	−5.641	−5.691			−5.276
E_b (eV)	−1.410	−1.423			−1.319
B (GPa)	240(1)	246(2)			245.5
B'	5.25(4)	5.66(4)			5.51
fcc			Ref. 60	MacFarlaine (Ref. 61)	$b_{ij}=0.4751$
V (Å^3)	15.91(2) [15.02]	15.58(3) [15.02]	15.02		15.02
a_o (Å^3)	3.992 [3.917]	3.965 [3.917]	3.917		3.917
r_b (Å^3)	2.823 [2.77]	2.803 [2.77]	2.770		2.770
E_{coh} (eV)	−5.77 [c]	−5.77 [c]	−5.77		−5.77
E_b (eV)	−0.962	−0.962	−0.962		−0.962
B (GPa)	260(2)	265(3)		288.4	282.6
B'	5.4(1)	5.9(2)			5.64

[a] Numbers given in brackets are rescaled to the experimental bond length in fcc-Pt.

[b] The bcc properties were calculated under the assumption of first-nearest-neigbor interaction. Later, the cutoff radius was chosen so that second-neighbor interaction occurs for bcc. This leads to a better agreement of the potential with the reference data.

[c] Value taken from experimental data.

the theoretical numbers. The ground-state oscillation frequency that determines β was set to 234 cm^{-1}, which again is close to the average of the literature values.

In the next step, the parameter S was adjusted by comparing Eq. (17) with the bond lengths and bond strengths of all reference structures. Figure 2 shows the corresponding plot in semi-logarithmic presentation. The properties of the diamond, sc and bcc phases follow almost a linear relationship. On the transition from bcc to fcc a significant deviation from this behavior occurs, which cannot be described within the present model. By connecting the data points of the fcc phase and the dimer, however, a reasonable agreement with all reference structures is achieved. Note that this line presents all mathematically possible minimum configurations for a given parameter set S, D_o, r_o, and β and is inpedendent of the analytical form and parametrization of $\overline{b_{ij}}$.

For comparison, data obtained with Baskes' modified embedded-atom potential (MEAM) (Ref. 7) are shown in the same plot. Obviously, the MEAM follows an almost linear relation as well, but predicts a significantly smaller change in bond lengths with varying coordination. In principle, a similar fit is also possible with the present bond-order potential but only at the expense of a realistic description of the dimer. Since possible applications of this potential may include simulation studies where dimer and cluster properties are of importance, we have chosen the parameter S that provides reasonable agreement with all reference data, including that for lower coordinations.

With the complete set of dimer parameters, the effective

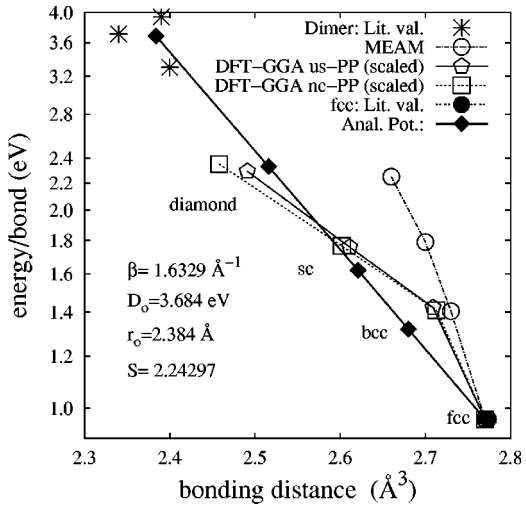

FIG. 2. Fit of the Pauling energy-bond relation to the Pt-dataset. Shown are the literature values of the dimer and fcc structure together with the results of nonlocal DFT calculations for diamond, sc,bcc and fcc structures. The bond lengths calculated from DFT have been rescaled to the experimental bond length in fcc-Pt. The analytical Pt potential is represented by the solid line. The open squares and diamonds show the nc-PP and us-PP DFT calculations, respectively. Open circles are the equilibrium energies and distances for the corresponding structures as calculated with the MEAM potential of Baskes (Ref. 7). Black squares indicate the corresponding minimum configurations of the different solid structures as calculated with the analytical potential.

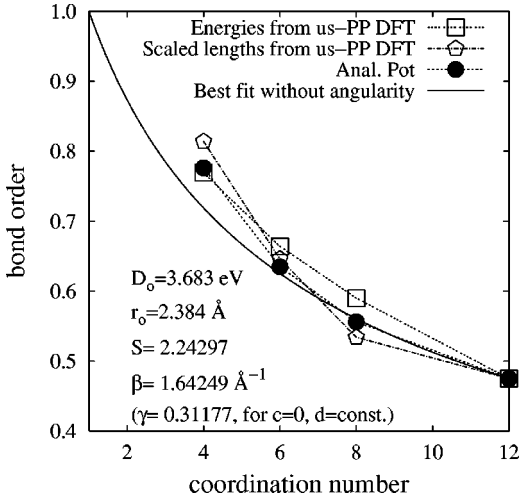

FIG. 3. Effective bond-order parameters as derived for the reference data from us-PP DFT calculations using Eqs. (19) and (20) compared with the analytically calculated bond-order. The solid circles describe the full potential including angularity, the solid line is the best fit of the bond-order without angular dependence.

bond order for the reference structures can be calculated directly either from the bond lengths, r_b, or energies, E_b, with the equations

$$\overline{b_{ij}} = (E_b/D_o)^{[1-(1/S)]} \tag{19}$$

and

$$\overline{b_{ij}} = \exp\{\beta[\sqrt{2/S} - \sqrt{2S}](r_b - r_o)\}. \tag{20}$$

Figure 3 shows the result for the energies and scaled bond lengths obtained from the us-PP DFT calculation. If angular dependencies are neglected ($c=0$), the parameter γ can be adjusted to the fcc phase, which allows the bond order to be

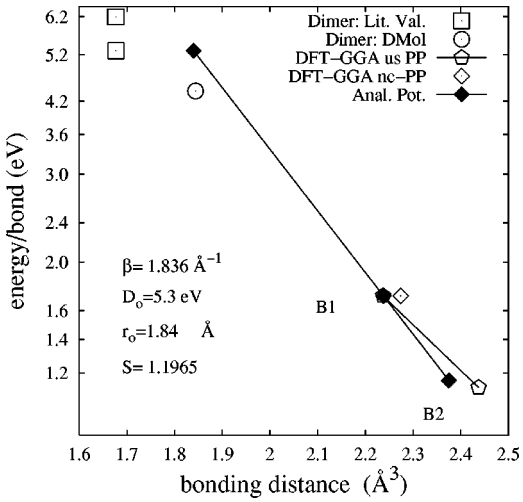

FIG. 4. Fit of the Pauling energy-bond relation to the Pt-C dataset. Open squares represent literature values for the Pt-C dimer properties, the open circle the Dmol result. The other open symbols show the DFT-results obtained by using us- and nc- pseudopotentials. The solid line with filled symbols refers to the analytical potential.

calculated as a simple function of coordination. Obviously, the square-root-dependent form is a reasonable approximation. It can be seen, however, that the analytically calculated values underestimate the bond–order for the lower coordinations if angularity is not included (see Fig. 4).

Therefore, the potential parameters determining the bond-order including angularity were also fit. In doing so, a numerical fitting scheme was applied that included the elastic properties in the reference data set. The resulting parameters are given in Table V. The analytically calculated effective bond order for the reference structures is now significantly improved by including the angular dependence as shown in Fig. 3. The cohesive properties of all structures compared to the DFT reference data are summarized in Table II. In general the numbers are in excellent agreement with the DFT results and experiments. For the sc and bcc phases, however, the absolute values of the cohesive energies are about 10% too small, which is a direct consequence of the bond order which only allows one to fit the bond lengths of these structures properly. Even the bulk moduli of all solid phases are very well reproduced, including the fcc phase, although none of them was part of the fitting procedure. This is a direct consequence of the proper choice for β which determines the curvature of the potential given by the dimer oscillation frequency. Additionally, B', the pressure derivative of the bulk modulus, which was calculated from the Birch-Murnaghan equation fits the numbers derived from total energies calculations very well. This is a significant result, since B' is directly related to the global Grüneisen parameter, and therefore a proper description of anharmonic effects can be expected from this potential. The most relevant properties of the fcc solid structure are summarized in Table III, and compared with established potentials for Pt.[4,5,7,22,40,41]

A noteworthy feature of the present model is the correct description of the elastic moduli. The inclusion of angularity makes possible anisotropy ratios smaller than two. The same is true for the MEAM, but all other models fail to reproduce this property. Only the calculated shear modulus c_{44} is somewhat too high, with the given parameter set. An alternative parameterization given in Appendix A does reproduce the

TABLE III. Materials properties of platinum as derived using the Pt potential of this work in comparison to experimental data and other Pt potentials. BO is the bond-order potential derived in this work, MEAM is the modified embedded-atom method of Baskes (Ref. 7), EAM is the embedded-atom potential as proposed by Foiles *et al.* (Refs. 4 and 40), OJ is the short-range potential by Oh and Johnson (Ref. 41), FS is the Finnis-Sinclair type potential of Sutton and Chen (Ref. 5), while TB means the empirical tight-binding potential of Cleri and Rosato (Ref. 22). Given are the cohesive energy per atom E_{coh}, lattice constant a_o, elastic moduli c_{ij}, bulk modulus B, pressure derivative of the bulk modulus B', Young's modulus C', anisotropy ratio c_{44}/C', melting point T_{melt}, vacancy formation energy $E_{f,\mathrm{vac}}$ and relaxation volume ΔV_{vac}, interstitial formation energy $E_{f,\mathrm{int}}$, and relaxation volume ΔV_{int} and surface energies E_s. Ω is the ideal atomic volume.

	Expt.	BO	MEAM	EAM	OJ	FS	TB
E_{coh} (eV)	5.77 (Ref. 60)	5.77	5.77	5.77	5.77	5.86	5.853
a_o (Å)	3.92 (Ref. 60)	3.92	3.92	3.92	3.92	3.92	3.924
c_{11} (GPa)	358 (Ref. 61)	351.5	347	303	312	314	341
c_{12} (GPa)	253 (Ref. 61)	248.1	251	273	268	258	273
c_{44} (GPa)	77.4 (Ref. 61)	89.5	76.9	68	63.3	74	91
B (GPa)	288.4 (Ref. 61)	282.6	283	283	283	277	296
B'	(5.4–5.9)[a]	5.52		5.64			
C' (GPa)	52.2 (Ref. 61)	51.6	48.06	15.0	22	28	34.0
c_{44}/C'	1.48 (Ref. 61)	1.73	1.6	4.53	2.88	2.64	2.68
T_{melt} (K)	2045 (Ref. 62)	2100(20)		1530 (Ref. 63)			1794(29) (Ref. 64)
$E_{f,\mathrm{vac}}$ (eV)	1.35 (Ref. 65)	1.21	<1.3[b]	1.68	1.48		1.17
$\Delta V_{\mathrm{vac}}/\Omega$	-0.2 (Ref. 66)	-0.33		-0.45			-0.73
$E_{f,\mathrm{int}}$ (eV)	3.5(6) (Ref. 67)	5.34		7.20[c]	4.67		
$\Delta V_{\mathrm{int}}/\Omega$	1.8 (Ref. 65)	1.86		2.18[c]			
E_s (eV/Å^2):							
(100)	0.114 (Ref. 42)	0.123	0.135	0.103			
(111)	0.092 (Ref. 42)	0.091	0.103	0.089			
(110)	0.243 (Ref. 42)	0.119	0.133	0.109			
(110)(2×1)		0.112					

[a]Results of DFT calculations.

[b]Calculated for an unrelaxed lattice.

[c]This value is the interstitial formation energy we have calculated for the {100} dumbell, which is the lowest-lying energy interstitial type in fcc metals. The values given by Foiles *et al.* (Ref. 40) (3.24 eV and $\Delta V_{\mathrm{int}}/\Omega = 1.4$) correspond to a tetrahedral defect position.

second order elastic constants, extremely well, but it does poorly in predicting the melting temperature.

The melting point was determined by monitoring the potential energy of an NPT ensemble containing both solid and liquid phases at a given temperature. For zero pressure we determined the temperature where the relative size of the two regions does not change, and therefore the average interface velocity is zero. We found that the melting point is mostly affected by the choice of the cutoff range, and therefore we adjusted the parameters R_{cut} and D using the known melting temperature of Pt. In doing so we calculated a melting point of 2100(20) K, which is in very good agreement with the experimental value of 2045 K. The fairly long range of the cutoff improves, at the same time, the description of the bcc structure since it now reaches the second-nearest-neighbor shell.

Defect properties were also examined. The relaxation volume of the interstitial fits the experimental number almost perfectly, but the formation energy is 5.31 eV compared to 3.5(6) eV obtained by experiment. Although this is a significant error, it is still an improvement over the energy of 7.46 eV obtained with Foile's EAM potential. Here it is worth noting that the number of 3.2 eV, as reported in Foiles original paper corresponds to a spurious defect structure and not to the [100] split interstitial. Both the calculated vacancy formation energy and the vacancy relaxation volume agree reasonably well with experiment. Even surface formation energies match recent DFT calculations.[42] The significant deviation for the (110) surface might be a consequence of neglecting atomic relaxations in the DFT calculations.

An important result gleaned from this study is that short-ranged bond-order potentials offer a realistic description of thermomechanical properties for Pt and potentially of other *d*-transition metals. The quality of the potential is at least comparable to the MEAM, and gives, in general, better agreement with reference data, both fitted and nonfitted, than the EAM models without angularity.

VI. PLATINUM-CARBON

Platinum and carbon do not form thermodynamically stable compounds, and consequently little information is available in the literature to guide the parameterization. The chemical interaction of Pt-C is mostly considered to be nonbonding, although this is only true when carbon bonds are fully saturated. There are many experiments, however, that are characterized by the chemical interaction of carbon and platinum. Cepek *et al.*[43] deposited fullerene clusters on Pt(111) surfaces, and found strong covalent bonds with very small charge transfer. Hecq *et al.*[44] reported the existence of a superficial compound $PtC_x(x \approx 1)$ in polycrystalline films of platinum containing up to 17% carbon that were synthesized by dc reactive sputtering. A superlattice structure of platinum-carbon was proposed by Westmacott, Dahmen, and Witcomb,[45] based on their observations of an ordered structure of Pt_7C in the vicinity of grain boundaries following quenching or irradiation. Finally, Shuvaev *et al.*[46] reported a six-fold coordinated Pt-C compound which was synthesized by co-evaporation of carbon and platinum and characterized by extended x-ray absorption fine-structure (EXAFS) analysis. Interestingly, experimental results on solid solubility of carbon in platinum are very inconsistent. While Siller *et al.*[47] reported solubilities of up to 4 atomic percent, Rut'kov and co-workers[48,49] suggested equilibrium concentrations that were three orders of magnitude smaller. Theoretical studies of solid Pt-C structures have, to our best knowledge, only been performed by Guillermet *et al.*,[50] who investigated the NaCl structure of $5d$ transition metals including PtC with a linear muffin-tin-orbital method.

In light of the sparse experimental information available, several DFT calculations were carried out to guide the fitting of the potential. For zinc-blende ($B3$), CsCl ($B2$), and NaCl ($B1$) structures with a stoichiometric basis of Pt and C atoms, bond distances as well as total energies were calculated. The cohesive energies were then determined using the the total energies from DFT calculations of pure carbon and platinum and the corresponding experimental cohesive energies.

The energetically most favored configuration is the NaCl lattice. For this structure the calculated bond length of 2.237 Å is somewhat higher than the value of 2.0 Å obtained from fitting EXAFS data. Shuvaev *et al.*[46] reported however, that the best experimental fit was achieved for coordination number six, which confirms our DFT result. For the same structure Guillermet *et al.*[50] calculated a bond length of 2.05 Å and a cohesive energy of -12.3 eV/f.u., which is about 2 eV lower than our value calculated with GGA-DFT (see Table IV).

Additional DFT calculations showed that the $B1$ and $B2$ phases of PtC are stable with respect to shear deformation, while zinc blende is not. The latter was therefore not considered for the potential fitting.

Dimer properties of platinum monocarbide are reported in Ref. 51 and in a much earlier paper by Singh *et al.*[52] The two calculations give consistent values for the bond lengths and oscillation frequencies, but they differ for the bonding energy. Since theoretical calculations on PtC dimer properties are not available, we additionally performed a DFT calculation using the code DMOL (Ref. 53) with BLYP (Ref. 54) functionals. In contrast to the literature values, the calculation predicts the $A^1\Pi$ state as the lowest lying energy configuration with significantly different dimer properties.

In order to fit the reference data, the parameter r_o was chosen in accordance to the DMOL calculations while D_o was adopted from Ref. 52. The parameter β was set so that both the bulk modulus of the $B1$ structure and the ground-state oscillation frequency are well reproduced. A comparison of the reference data with the predictions of the analytical potential is given in Table IV). The corresponding potential parameters are listed in Table V. Although this parameter set reproduces the essential features of the Pt-C interaction, it is based on a minimal set of input data and therefore might need to be refitted if more detailed reference data become available.

VII. CONCLUSIONS

We present an analytical potential that allows us to model chemical bonding in mixed metallic-covalent systems using

TABLE IV. Calculated structural and cohesive properties of Pt-C in various hypothetical phases: volume per formula unit V, lattice constant a_o, cohesive energy per formula unit E_{coh}/atom, cohesive energy per bond E_b, and pressure derivative of bulk modulus B'. Compared are results of DFT calculations within the GGA using CASTEP with ultrasoft pseudopotentials and density mixing (us-PP), as well as Troullier-Martins pseudopotentials with all band minimalization (nc-PP).

Pt-C	CRC (Ref. 51)	Singh (Ref. 52)	Dmol	Anal. Pot.
r_b (Å^3)	1.6767	1.677	1.844	1.84
E_{coh}/f.u. (eV)		5.3	4.4	5.3
E_b (eV)	6.2	5.3	4.4	5.3
ω_o (cm^{-1})	1051.13	1051.18	706	928
$B1$ (NaCl)	nc-PP	us-PP	LMTO (Ref. 50)	$b_{ij}=0.8306$
V (Å^3/f.u.)	22.712(11)	22.405(3)	18.58	22.41
a_o (Å^3)	4.495	4.475	4.205	4.476
r_b (Å^3)	2.274	2.237	2.1	2.238
E_{coh}/f.u. (eV)	−10.271	−10.266	−12.67	−10.271
E_b (eV)	−1.711	−1.711	−2.11	−1.711
B (GPa)	261(1)	271(1)		274
B'	4.96(4)	4.95(5)		4.87
$B2$ (CsCl)				$b_{ij}=0.7790$
V (Å^3/f.u.)		22.29(3)		20.62
a_o (Å^3)		2.814		2.742
r_b (Å^3)		2.437		2.375
E_{coh}/f.u. (eV)		−8.973		−9.27
E_b (eV)		−1.122		−1.159
B (GPa)		240(1)		291
B'		5.22(4)		4.94

a single functional form. Our model makes use of the insight that chemical bonding of most covalent systems and *d*-transition metals can be described within a second-momentum tight-binding approach. We show that the original version of Brenner's carbon potential can be used for modeling Pt as well as Pt-C if angular contributions are included. This ansatz can have an tremendous importance for atomic scale computer simulations of a wide class of materials problems where bonding interactions between covalent and metallic systems are important. Due to the limited number of adjustable parameters the model allows a systematic fit of materials properties.

TABLE V. Parameter set of the relevant interaction types. All parameters are pair type dependent.

	Pt-Pt	Pt-C	C-C
γ	$8.542\times10-4$	9.7×10^{-3}	2.0813×10^{-4}
S	2.24297	1.1965	1.22
β (Å^{-1})	1.64249	1.836	2.1
D_o (eV)	3.683	5.3	6.0
r_o (Å)	2.384	1.84	1.39
c	34.00	1.23	330
d	1.1	0.36	3.5
2μ (Å^{-1})	2.67	0.0	0.0
R_{cut} (Å)	3.1	2.65	1.85
D (Å)	0.2	0.15	0.15

[a]If simulations of amorphous structures are intended, a modified cutoff range should be used (Ref. 68).

ACKNOWLEDGMENTS

This work was supported by the U.S. Department of Energy through the University of California under Subcontract No. B341494 and by the U.S. Department of Energy, Basic Energy Sciences, under Grant No. DEFG02-96ER45439. Grants of computing time from National Computational Science Alliance at UIUC and the National Energy Research Supercomputer Center are gratefully acknowledged.

APPENDIX A: ALTERNATIVE PARAMETER SET FOR PLATINUM

In the course of this study several parameterizations were tested, mostly due to the uncertainties in the dimer parameters. With $D_o=3.71$ eV, $r_o=2.34$ Å, $\beta=1.65921$ Å^{-1}, $\gamma=2.643\times10^{-4}$, $S=1.79493$, $c=21.36$, $d=0.589$, $2\mu=2.69$ Å^{-1}, $R_{cut}=3.1$ Å, $D=0.2$ Å, improved elastic properties were found for platinum ($c_{11}=258.9$ GPa, $c_{12}=253.4$ GPa, and $c_{44}=81.0$ GPa). The vacancy formation energy, however, is only 0.74 eV, and the melting point goes

to about 1500 K, while surface energies and interstitial formation energy (4.05 eV) are still in very good agreement with the reference data. Even the simplified version without angularity ($c=0$, $\gamma=0.20967$, $R_{cut}=3.4$ Å, and $D=0.2$ Å) delivers a reasonable description of most properties except for the surface properties and might be useful for the quantification of models that rely on bond counting.

APPENDIX B: MODIFICATION OF THE REPULSIVE POTENTIAL

In applications where one needs to take high-energetic ($E_{kin} \gg 10$ eV) collisions between atoms into account, it is necessary to modify the repulsive part of the potential to realistically describe such collisions. To this end, we first derive an accurate repulsive pair potential for a dimer using a density-functional theory method. We then construct a total potential V_{Tot} using

$$V_{Tot}(r) = V_R(r)[1-F(r)] + [V_{Eq}(r)]F(r), \qquad \text{(B1)}$$

where V_{Eq} is the potential for states close to equilibrium described in the main text, and the Fermi function

$$F(r) = \frac{1}{1+e^{-b_f(r-r_f)}}. \qquad \text{(B2)}$$

The value of the constants b_f and r_f are chosen such that the potential is essentially unmodified at the equilibrium and longer bonding distances, and that a smooth fit at short separations with no spurious minima is achieved for all realistic coordination numbers.

Using this approach we obtained $r_f=1.5$ Å and $b_f=10.0$ 1/Å for the Pt-Pt interactions, and $r_f=0.7$ Å and $b_f=9.0$ 1/Å for C-C interaction as well as $r_f=0.8$ Å and $b_f=8.0$ 1/Å for Pt-C interactions. These same values also give a smooth fit to the Ziegler-Biersack-Littmark universal repulsive potential.[55]

*Author to whom correspondence should be addressed. Present address: Institut für Materialwissenschaft, TU Darmstadt, Petersenstr. 23, D-64287 Darmstadt, Germany. Email address: albe@tu-darmstadt.de

[1] M. Daw and M. Baskes, Phys. Rev. Lett. **50**, 1285 (1983).
[2] M. Daw and M. Baskes, Phys. Rev. B **29**, 6443 (1984).
[3] M. Finnis and J. Sinclair, Philos. Mag. A **50**, 45 (1984).
[4] S. Foiles, M. Baskes, and M. Daw, Phys. Rev. B **33**, 7983 (1986).
[5] A. Sutton and J. Chen, Philos. Mag. Lett. **61**, 139 (1990).
[6] J. Tersoff, Phys. Rev. B **49**, 16 349 (1994), and references therein.
[7] M. Baskes, Phys. Rev. B **46**, 2727 (1992).
[8] S. Liem and K.-Y. Chan, Surf. Sci. **328**, 119 (1995).
[9] H. Rafii-Tabar, H. Kamiyama, and M. Cross, Surf. Sci. **385**, 187 (1997).
[10] H. Rafii-Tabar, Acta Phys. Pol. A **93**, 343 (1998).
[11] S. Caroll, S. Hall, R. Palmer, and R. Smith, Phys. Rev. Lett. **81**, 3715 (1998).
[12] R. Chatterjee, Z. Postawa, N. Winograd, and B. Garrison, J. Phys. Chem. B **103**, 151 (1999).
[13] W. Harbich, S. Fedrigo, and J. Buttet, Z. Phys. D: At., Mol. Clusters **26**, 138 (1993).
[14] L. Bardotti, P. Jensen, A. Hoareu, M. Treilleux, and B. Cabaud, Phys. Rev. Lett. **74**, 4694 (1995).
[15] J. Bernholc, C. Roland, and B. Yakobson, Curr. Opin. Solid State Mater. Sci. **2**, 706 (1997).
[16] M. Boudart, Nature (London) **372**, 320 (1994).
[17] Z. Xu, F.-S. Xiao, S. Purnell, O. Alexeev, S. Kawi, S. Deutsch, and B. Gates, Nature (London) **372**, 357 (1994).
[18] K. Yamashita, O. Matsudo, J. Yamazaki, I. Hatsukade, T. Ishigami, S. Takahama, K. Tamura, and M. Ohtani, Rev. Sci. Instrum. **63**, 1217 (1992).
[19] *Phase Equilibria of Binary Alloys*, Landolt-Börnstein, New Series, edited by O. Madelung, Group IV, Vol. 5b (Springer-Verlag, Berlin, 1992).
[20] F. Ducastelle, J. Phys. (Paris) **31**, 1055 (1970).
[21] J. Friedel, in *Physics of Metals. 1. Electrons*, edited by J. Ziman (Cambridge University Press, Cambridge, 1969), Chap. 8, p. 340.
[22] F. Cleri and V. Rosato, Phys. Rev. B **48**, 22 (1993).
[23] G. Abell, Phys. Rev. B **31**, 6184 (1985).
[24] D. Brenner, Phys. Rev. Lett. **63**, 1022 (1989).
[25] D. Brenner, Phys. Rev. B **42**, 9458 (1990).
[26] K. Khor and S.D. Sarma, Phys. Rev. B **38**, 3318 (1988).
[27] P. Alinaghian, S. Nishitani, and D. Pettifor, Philos. Mag. B **69**, 889 (1994).
[28] D. Conrad and K. Scheerschmidt, Phys. Rev. B **58**, 4538 (1998).
[29] I. Oleinik and D. Pettifor, Phys. Rev. B **59**, 8500 (1999).
[30] D. Pettifor, *Bonding and Structure of Molecules and Solids* (Oxford Science Publications, Oxford, 1995).
[31] R. O. Jones and O. Gunnarsson, Rev. Mod. Phys. **61**, 689 (1989).
[32] M. Payne, M. Teter, D. Allen, T. Arias, and J. Joannopoulos, Rev. Mod. Phys. **64**, 1045 (1992).
[33] N. Troullier and J. Martins, Solid State Commun. **74**, 613 (1990).
[34] J. Perdew and Y. Wang, Phys. Rev. B **45**, 13 244 (1992).
[35] D. Ceperley and B. Alder, Phys. Rev. Lett. **45**, 566 (1980).
[36] J. Perdew and A. Zunger, Phys. Rev. B **23**, 5048 (1981).
[37] F. Birch, J. Geophys. Res. **83**, 1257 (1978).
[38] K. Albe, Phys. Rev. B **55**, 6203 (1997).
[39] J. Furthmüller, J. Hafner, and G. Kresse, Phys. Rev. B **50**, 15 606 (1994).
[40] S. Foiles, M. Baskes, and M. Daw, Phys. Rev. B **37**, 10 378 (1988).
[41] D. Oh and R. Johnson, J. Mater. Res. **3**, 471 (1988).
[42] P. van Beurden and G. Kramer, Phys. Rev. B **63**, 165106 (2001).
[43] C. Cepek, A. Goldoni, and S. Modesti, Phys. Rev. B **53**, 7466 (1996).
[44] A. Hecq, T. Robert, M. Hecq, J. Delrue, J. Pireaux, and R. Caudano, J. Less-Common Met. **80**, P83 (1981).
[45] K. Westmacott, U. Dahmen, and M. Witcomb, Metall. Trans. A **17**, 807 (1986).
[46] A. Shuvaev, P. Ovysannikov, and T. Luyebeznova, Physica B **209**, 571 (1995).
[47] R. Siller, W. Oates, and R. McLellan, J. Less-Common Met. **16**, 71 (1968).

[48] E. Rut'kov, Zh. Tekh. Fiz. **63**, 122 (1993) [Techn. Phys. **38**, 220 (1993)].
[49] E. Rut'kov and A. Tontegode, Fiz. Tverd. Tela (Leningrad) [Sov. Phys. Solid State **38**, 351 (1996)].
[50] A. Guillermet, J. Häglund, and G. Grimwall, Phys. Rev. B **48**, 11673 (1993).
[51] *CRC Handbook of Chemistry and Physics*, 81st ed., edited by R. Weast and D. R. Lide (CRC Press, Boca Raton, FL, 2001).
[52] O. Singh and B. Asthana, Acta Phys. Pol. A **51**, 575 (1977).
[53] DMOL 96.0/4.0 User Guide, Molecular Simulations, San Diego, 1996.
[54] C. Lee, W. Yang, and R. Parr, Phys. Rev. B **37**, 785 (1988).
[55] J. Ziegler, J. Biersack, and U. Littmark, *The Stopping and Range of Ions in Solids* (Pergamon, New York, 1985).
[56] S. Yang, D. Drabold, J. Adans, P. Ordejon, and K. Glassford, J. Phys.: Condens. Matter **9**, L39 (1997).
[57] S. Varga, B. Fricke, H. Nakamatsu, T. Mukoyama, J. Anton, D. Geschke, A. Heitmann, E. Engel, and T. Bastug, J. Chem. Phys. **112**, 3499 (2000).
[58] S. Taylor, G. Lemire, Y. Hamrick, Z. Fu, and M. Morse, J. Chem. Phys. **89**, 5517 (1988).
[59] S. Gupta, B. Napti, and K. Gringerich, Inorg. Chem. **20**, 966 (1981).
[60] *Metal Reference Book*, edited by C. Smith (Butterworths, London, 1976).
[61] R. MacFarlaine, Phys. Rev. Lett. **18**, 91 (1965).
[62] C. Kittel, *Introduction to Solid State Physics*, 5th ed. (Wiley, New York, 1976).
[63] K. Nordlund, M. Ghaly, R.S. Averback, M. Caturla, T. Diaz de la Rubia, and J. Tarus, Phys. Rev. B **57**, 7556 (1998).
[64] L. G'omez, A. Dobry, and H. Diep, Phys. Rev. B **55**, 6265 (1997).
[65] *Atomic Defects in Metals*, edited by H. Ullmaier, Londolt-Börnstein, New Series, Group III, Vol. 25 (Springer, Berlin, 1992), p. 257.
[66] P. Ehrhart, K. H. Robrock, and H. R. Schober, in *Physics of Radiation Effects in Crystals*, edited by R. A. Johnson and A. N. Orlov (Elsevier, Amsterdam, 1986), p. 3.
[67] W. Schilling, J. Nucl. Mater **69&70**, 465 (1978).
[68] H. Jäger and K. Albe, J. Appl. Phys. **88**, 1129 (2000).